

JOURNAL OF TECHNIQUES

Journal homepage: http://journal.mtu.edu.iq



RESEARCH ARTICLE - MECHANICAL ENGINEERING

Study of Four-Stroke Engine Vibrations: Influence of Friction and Thermal Effects on Piston Speed, Displacement, and Acceleration

Hayder Mohammed Mnati¹, Maroua Hammami^{1, 2*}, Olfa Ksentini^{1, 3}, Mohamed S. Abbes¹

¹Laboratory of Mechanics, Modelling and Manufacturing (LA2MP), National Engineering School of Sfax, Ministry of Higher Education and Research of Tunisia, Sfax, Tunisia

²National School of Engineers of Carthage, University of Carthage, 2035 Charguia II Tunis, Tunisia ³University of Gabes, Higher Institute of Industrial Systems of Gabes (ISSIG), Gabes, Tunisia

* Corresponding author E-mail: hammamimaroi@gmail.com

Article Info.	Abstract
Article history:	This paper presents an analysis of vibrational influences on the stability of four-stroke IC engines (Internal Combustion)
Received 31 May 2025	by comparing different engine types to determine the engines most sensitive to increased values of vibrations. Emphasis is given to single-cylinder engines in particular to a popular motorcycle engine that was found to generate the highes vibration levels ever obtained. Vibration measurements were made at engine points on the engine for experimenta evaluation of the stability and dynamics of the engine under varied operating conditions. Analog accelerometer modules
Accepted 28 August 2025	were integrated into the engine and tied to an Arduino-based control system that allowed to get on the spot results whenever wanted. A modal analysis using MATLAB was conducted to study the effects of connecting rod length or essential performance characteristics based on acceleration, velocity and displacement. The results show that using longe
Publishing 30 September 2025	rods results in lower levels of vibrations, which illustrates that rod length is an important parameter in relation to the vibration properties. This study provides valuable insights into vibration mitigation strategies aimed at enhancing the reliability, efficiency, and overall performance of internal combustion engines. The highest vibration at low acceleration was recorded at 1500 rpm with a value of 16 mm/s², while the highest vibration at high acceleration occurred at 1900 rpm reaching 33.4 mm/s². Numerical analysis of the slider-crank mechanism dynamics (r = 26 mm, L = 130 mm) using
	MATLAB shows that friction reduces velocity, acceleration, and displacement by 15% across all rod lengths. Additionally temperature effects reduce acceleration by 8.5%, and the combined influence of friction and temperature leads to a 22% reduction in velocity, acceleration, and displacement. In comparison to other engines, the Toyota 6-cylinder engine is among the most dependable, low-vibration, and long-lasting. The Toyota 2500 and BOXER 150CC engines displayed the lowest vibrations (1.4 mm/s ² at 800 rpm), suggesting exceptional stability.

This is an open-access article under the CC BY 4.0 license (http://creativecommons.org/licenses/by/4.0/)

Publisher: Middle Technical University

Keywords: Crank; Kinematics; Internal Combustion Engine; Connecting Rod; Vibration Signal Analysis.

1. Introduction

An engine is a propulsion device that converts a specific form of energy into mechanical work. Internal combustion engines (ICEs), particularly four-stroke engines, are among the most widely used types of thermal engines in modern applications such as automobiles, motorcycles, agricultural machinery, and portable equipment [1]. These engines are designed to generate rotational motion by combusting fuel-air mixtures, thereby producing power to overcome external resistances and perform useful work. Despite their broad utility, internal combustion engines are subject to vibrational forces, which arise primarily from the reciprocating motion of internal components and the combustion process itself [2]. Vibrations of reciprocating internal combustion engine do not only result from its operating, but they have significant influence on engine operation, efficiency and durability. Built-up vibration can cause mechanical parts to fail early, maintenance costs to increase and driver comfort to decrease. In single-cylinder engines, typically used in motorcycles and small machines, vibration is exacerbated by the lack of phase-shifted cylinders for inertia force balancing [3]. It is therefore important to analyze the sources and effects of vibration in axial piston machines, with the aim of optimizing the performance and improving the design of such machines.

Numerous developments have been carried out to minimize ICE vibration by improving structural design and analysis. The crank-slider mechanism, including the piston, connecting rod, crankshaft, and bearings, is a main driver of engine vibration. The mechanical configuration and notably the connecting rod length, influence motion properties like speed, acceleration, and elongation. These, of course, dictate the magnitude of inertia 1 forces within engine [4]. Kinematic analysis is a complex study that theories dynamics of the engine, in which each motion parameter of the piston - crank mechanism can be expressed as a function of the crank - angle. This area has been covered by a few investigators. Mnati et al. (2025) the natural frequencies of the engine were calculated, which was used to locate possible resonance conditions

Nomenclature & Symbols					
PRO-E	Pro/ENGINEER	TDI	Turbocharged Direct Injection		
MSC	MSC Software / MSC Nastran	В	Biodiesel Blends		
FEA	Finite Element Analysis	EGR	Exhaust Gas Temperature		
IC	Internal Combustion	BSFC	Brake Specific Fuel Consumption		

at different engine speed and load conditions [5]. Piston and connecting rod speed and velocity were obtained via crank angle derivative by Nigus (2015) [6] and software analysis focused on computing piston motion, velocity, and acceleration according to crankshaft rotation was reported by Lučić (2022) [7]. Xiang [1] also stressed that combustive noise in ICEs is usually covered by other noise sources of mechanical and aerodynamic, and conventional detecting methods are always lack for singling out vibroacoustic of combustive origin.

As an example, related to the design optimisation, Niusha et al. (2021) [8] proposed balancer utilization significantly helped to reduce the vibration a systematic procedure to design and analyze pistons of a four-stroke engine by employing ANSYS workbench technique to estimate the mechanical normalcy for the operational loads. M.Viswanath et al. (2021) [9] proposed a model to simulate how to the Piston plays a main role in energy conversion. Failure of piston happens due to various thermal in software like PRO-E (Pro-engineer) and ANSYS which provide higher performance with reduced weight. Zhang and Wu (2014) investigated the thermo-mechanical coupling of diesel engine piston and found that temperature played a leading role in the influence on the piston stress and deformation [10]. This observation is consistent with the general understanding that thermal effect plays an important role in controlling vibration in reciprocating engines. Other work Stress and fatigue of engine components have been also analyzed by other researchers. Pham et al. (2017) analysed the stress distribution in reciprocating compressors pistons and connecting rods and found that the presence of high steresses concentrations allows for acceptable level of safety of operation [11]. Ranjbarkohan (2010) studied the fault mode effects and criticality analysis of the Nissan Z24 engine, indicating the loose of crankshaft and connecting rod due to over downshifting and the life of high rotary per minute (RPM) [12]. The dynamic performances of the slider-crank mechanism were fully investigated on MSC Adams (MSC Software / MSC Nastran). In another investigation, fatigue life of motorcycle connecting rods was studied by Horváth and Égert (2015) who have combined the use of FEA (Finite Element Analysis) coupled with experimental validation to compare the fatigue performance of the existing and improved rod designs under cyclic loading [13].

A further domain under consideration is vibration isolation and damping. Alkhatib and Dhingra (2013) optimized the stiffness, orientation and placement of elastomeric engine mounts using a parametric method [14]. Their finite element analysis contributed to a new and better engine mount design that reduced the transmission of vibration. Beckers et al. [3] altered to incorporate spring-damper element in a slider-crank yielded lesser transmitted loads and better performance during the resonance condition while applying act-and-wait control [15]. Chen et al. modelling the impact of over-dimension clearance in big-end bearing, by modifying conventional kinematic relations and using the Reynold's equation for a more accurate prediction of the bearing forces [16]. Next, recent developments that have enriched the computational arsenal available to support engine performance modeling and simulation are discussed. Zheng et al. (2021) used deep neural networks combined with virtual sample generation for more accurate and cost-effective prediction of marine diesel engine performance [17]. Armentani et al. (2018) employed powertrain dynamics to look at vibration characteristics within turbocharged diesel engines with a focus on damping and moment of crank shaft angular velocity change [18]. Madamedon (2018) presented IAS models for diagnosing faults in a diesel engine and demonstrated the sensitivity of low-frequency resonances to common problems like misfires [19]. Tailony (2018) later proposed a lumped mass model for torsional analysis and was able to predict the driveline natural frequencies to a high degree of accuracy [20]. Yu et al. (2019) developed a 3D dynamic model of a single-cylinder crank and connecting rod mechanism in ADAMS/VIEW software [4]. They were able to reduce inertiainduced vibrations substantially by using a uniaxial balancing technique and a balance shaft. Finally, Consuegra et al. (2019) developed a method of real-time in-cylinder volume calculation to account for variations, increasing the precision of both the combustion and vibration model [3]. Beside that Zanganeh and Soleiman (2021) [21] added that drivers experiencing mechanical vibrations may face health problems such as backaches and spinal injuries. Tractors without chassis use a balancer unit to reduce secondary engine vibrations, which reduces vibration by 22.3%, especially at higher rotational speeds under full load conditions. According to Liss et al. (2024) [22] The study showed that the 1.2 TDI (Turbocharged Direct Injection) engine generated higher vibration amplitudes and more variable frequencies than the 1.6 TDI, negatively affecting overall driving comfort. Moreover, Marwa and Salih, 2020 [23] presented that Biodiesel blends (B20, B30, B50) reduced CO (Carbon Monoxide), HC (Hydrocarbons), and EGT (Exhaust Gas Temperature) but increased BSFC (Brake Specific Fuel Consumption) and NOx, (Nitrogen Oxides) with B20 showing only minor efficiency loss (4%) and best emission balance. Thus, B20 is the optimal blend for unmodified diesel engines [24]. In addition to that (Marzec and Kubica 2024). The study looks at how LPG/DME fuel mixes affect a sparkignition engine's dynamic performance. Even if a greater DME component (30%) decreases acceleration at maximum loads. Notable (Oskari et al. 2024) [25] the same idea by contrasting two approaches to describe combustion in diesel engines: the instantaneous mean frequency variation of the signal and the study of the cylinder pressure time signal [26]. However, Noga and Mareczek (2020). found that increasing hybrid fuels can churn noise and vibration that negatively affected both passenger comfort and driver well-being. As much promise as hybrid and natural gas fuels hold, their challenges mean they still baseline for the engines, which are being transitioned to lower-cylinder configurations, maintain power and torque. Similarly, Daud et al. (2023) [27] provided appropriate alcohol and making alternative fuel mixes can enhance engine performance, improve fuel efficiency and reduce harmful emissions and vibration. Building on Chen's et al, (2025) [28] study show that a dynamic similarity method for aero-engine rotors based on evolutionary algorithms is developed, matching the prototype's first three critical speeds with relative error of 0.95%, 0.98%, and 0.28%. Effective vibration control is supported by the simplified rotor model, which accurately replicates vibration patterns. In the same way Kwaku et al. (2023) [29] suggest that to minimize weight without sacrificing strength, this study examines the viability of designing connecting rods out of AA (aluminium alloy)7075. AA7075 was compared to titanium alloy, grey cast iron, and structural steel using modal and thermal studies. According to the results, AA7075 outperformed the other materials in terms of natural frequency, total heat flux, and weight reduction potential, but it also had the largest deformation and 0.95%, 0.98%, and 0.28% relative errors in matching critical speeds. In the same side Sena et al. (2021) [30] tested gasoline blended with 15% ethanol, ethyl octanoate, or ethyl oleate in a 4-stroke engine at 4400 rpm, showing similar hourly fuel consumption to pure gasoline. Ester blends also improved brake specific fuel consumption at higher loads, indicating better energy conversion efficiency.

In this context, some experimental and numerical studies were carried out in the last years that analyzed together the experimental and numerical points of view of the vibrations in internal combustion engines, especially the combined effect of the structural design configuration, lubrication and thermal conditions. This discovery gives rise to the need to investigate and compare vibration responses in single, four and six-

cylinder four stroke engines, concentrating on determining which one of these has the highest risk of suffering performance loss due to vibrations. This was achieved by conducting experimental vibration measurements on an actual single-cylinder engine in a real-time environment, with analog accelerometers connected to an Arduino based system. Modal analysis, focusing on the effect of the length of the connecting rod on motions (i.e. acceleration, velocity, and displacement) were conducted using MATLAB. Additionally, the study explores the impact of friction (representing lubrication effects) and temperature variations on engine dynamics through a detailed numerical analysis of the slider-crank mechanism.

The novelty of this study lies in its hybrid experimental-simulation methodology and its comprehensive evaluation of how structural and environmental factors, specifically connecting rod length, lubrication, and temperature, affect vibration characteristics in internal combustion engines. By bridging experimental observations with computational modelling, this research provides actionable insights into vibration mitigation strategies that can enhance engine performance, reliability, and durability, especially in lightweight and compact engine systems such as those used in motorcycles and small machinery.

2. Methodology

2.1. Experimental setup

This study analyzes and assesses the vibrations of various four-stroke engines, to determine which engine type is most prone to high vibration levels. As shown in Fig. 1, the results indicate that a specific Chinese single-cylinder motorcycle engine exhibits the highest vibration levels among the engines tested. To address this issue, several experimental investigations were conducted to evaluate the effect of low-octane fuel on vibration intensity. Measurements of engine structural vibrations using a vibration meter revealed complex signals resulting from the interaction of multiple vibration sources, each influenced by its own transmission path. Elevated vibration levels were attributed to several internal engine phenomena, including fluctuations in combustion pressure and imbalance between rotating and reciprocating components.

The engine was tested at speeds of 800, 1100, 1500, and 1900 rpm under ambient conditions of 25 °C and 30% relative humidity. A programmed Arduino Uno board was attached to two sensors placed close to the crankshaft and the piston to acquire vibrations in three axes (x, y, z). They included a Grove 3-Axis analog accelerometer (ADXL335) specifications as shown in Table 1 and an Arduino-Uno-Rev3 (R3) board. In this construction the analog outputs (X, Y and Z) of the accelerometer were linked to the (A0, A1 and A2) analog input pins of the Arduino and the power and ground pins were connected to 5V and GND of Arduino, respectively. This arrangement allowed the data to be collected perfectly and improved the repeatability of the measurements.

The Grove 3-Axis Analog Accelerometer specifications as shown in Table 2. is an integrated 3-axis accelerometer with a signal conditioned analog voltage output using capacitive sense technology, maintaining the analog voltage output at specific acceleration levels over time. The accelerometer has a full-scale range of ± 3 g with a sensitivity of 270–330 mV/g, and is suitable for operation within the voltage range of 1.8 V to 3.6 V (recommended 3.3 V) and the temperature range of ± 40 °C to ± 85 °C. The Arduino Uno R3 uses the ATmega328P microcontroller and has a frequency of 16 MHz and is programmable using a standard USB interface. It has a maximum sampling rate of around 10 kHz in analog and ideal for low number of channels (like vibration measurement).

Data acquisition process: There were several steps to acquire the vibration data

- Signal Input: The accelerometer provides an analog voltage to represent the acceleration on each axis. These signals are read by the Arduino's analog input pins (A0, A1, A2).
- Analog-to-Digital Conversion (ADC): The Arduino's built-in ADC converts the analog signals into 10-bit digital values ranging from 0 to 1023.
- Acceleration Calculation: A predefined algorithm converts the digital values into acceleration measurements (in g-force), based on the
 accelerometer's sensitivity (mV/g).
- Data Output: The Arduino either stores the processed data or transmits it via serial communication to a connected computer or display for further analysis.

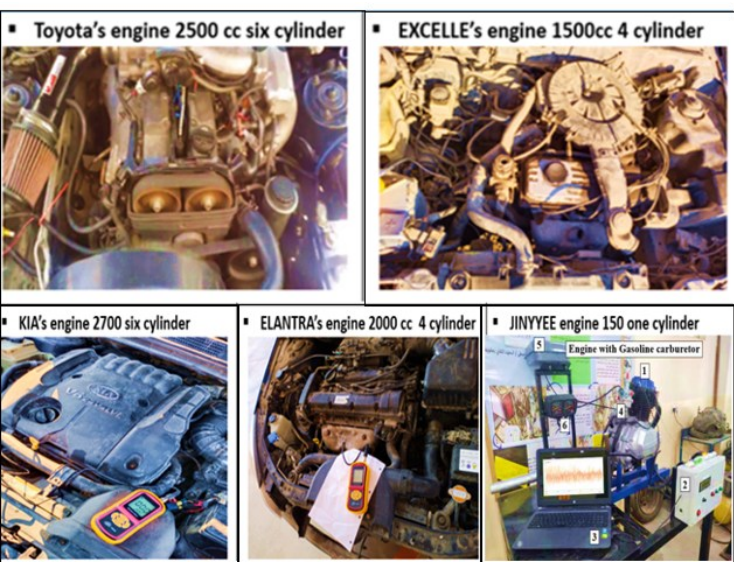


Fig. 1. Types of tested engines

Table 1. Specifications of the Arduino Uno Rev3 (R3)

Category	Specification	Tolerance
Microcontroller	ATmega328P (8-bit AVR)	±0% (fixed)
Operating Voltage	5V	±5% (4.75-5.25V)
Input Voltage	7–12V (recommended), 6–20V (limits)	$\pm 10\%$ at max limits
Digital I/O Pins	14 (6 provide PWM)	±0% (fixed)
PWM Pins	6 (D3, D5, D6, D9, D10, D11)	$\pm 0\%$ (fixed)
Analog Input Pins	6 (A0–A5)	±0% (fixed)
DC Current per I/O Pin	20 mA	±5% (19-21mA)
Flash Memory	32 KB (0.5 KB used by bootloader)	±0% (fixed)
SRAM	2 KB	±0% (fixed)
EEPROM	1 KB	±0% (fixed)
Clock Speed	16 MHz (crystal oscillator)	$\pm 0.5\%$
USB Interface	USB Type-B (with ATmega16U2 for serial communication)	±0% (fixed)
UART	1 (via ATmega328P and ATmega16U2)	±0% (fixed)
SPI	Yes (D10–D13: SS, MOSI, MISO, SCK)	±0% (fixed)
I^2C	Yes (A4: SDA, A5: SCL)	±0% (fixed)
Dimensions	$68.6 \text{ mm} \times 53.4 \text{ mm}$	±0.5 mm
ICSP Header	2 (1 for ATmega328P, 1 for ATmega16U2)	$\pm 0\%$ (fixed)
Power Pins	5V, 3.3V, GND, Vin	$\pm 5\%$ for voltage
Analog Reference	AREF pin for external reference voltage	$\pm 1\%$
Reset Button	Yes	±0% (fixed)
LED Indicators	Power (ON), TX/RX (serial), L (D13) $\pm 0\%$ (fix	
Weight	~25 g	±2 g

Table 2. Technical specifications of accelerometer

Parameter	Specification		
Module symbol	Grove - 3-Axis Analog Accelerometer - ADXL335		
Accelerometer	ADXL335		
Working principle	Capacitive Voltage, analog		
Output type			
Range	±3g (Full Scale)		
Sensitivity	270 to 330 mV/g		
Operating voltage	1.8V - 3.6V (3.3V Suggested)		
Temperature range	−40 to +85°C		

This configuration, managed through code developed in the Arduino IDE, enabled continuous vibration monitoring, visualization, and potential triggering of specific actions based on vibration thresholds.

A vibration meter was also used to verify and monitor vibration levels at various engine speeds, measuring acceleration (A), velocity (V), and displacement (X). The key findings are as follows:

- At 1500 rpm, the maximum vibration under low acceleration was measured at 16 mm/s².
- At 1900 rpm, the highest vibration at high acceleration reached 33.4 mm/s².
- Displacement and velocity peaked at 1500 rpm, with values of 0.044 mm and 5.2 mm/s, respectively.

Table 3 summarizes the recorded vibration data at the various engine speeds.

Table 3. Results of T engines vibration

Engine Type	Speed	Low Acceleration (A)	High Acceleration (A)	Velocity (V)	D'andreas (W)
Engine Type	(rpm)	mm/s²	mm/s²	mm/s	Displacement (X) mm
	800	2.0	2.5	6.8	0.104
Toyota 2500	1100	1.5	4.0	4.1	0.1
(6-cyl)	1500	1.9	2.1	2.7	0.65
	1900	3.2	2.3	3.5	0.064
	800	1.4	2.7	2.0	0.62
IZIA 2700 (C aml)	1100	3.2	6.6	2.3	0.051
KIA 2700 (6-cyl)	1500	5.2	12.1	2.1	0.04
	1900	7.7	15.6	2.5	0.036
	800	3.7	3.9	12.2	0.191
EXCELLE 1500	1100	6.1	8.5	6.4	0.066
(4-cyl)	1500	7.7	13.6	6.7	0.055
(-3)	1900	9.1	18.1	7.3	0.063
	800	3.6	7.1	6.5	0.087
ELANTRA 2000	1100	3.8	10.6	7.3	0.099
(4-cyl)	1500	4.4	9.2	9.9	0.119
(-3)	1900	5.8	11.3	3.2	0.083
	800	0.33	5.1	1.3	0.025
JINYYEE 150 (1-	1100	8.4	11.4	2.7	0.034
cyl)	1500	16.0	23.2	5.2	0.044
- J - J	1900	13.7	33.4	3.0	0.017

2.2. Experimental procedure

This paper intends to assess the vibration limits of several four-cycle engines and compare them in relation to high vibration. In Figs. 2–7, parameters such as acceleration (A), velocity (V) and displacement (X) were measured at different speeds of the engine with the help of a vibration meter. Maximum low acceleration vibration recorded at 16mm/s² at 1500 RPM. The highest high acceleration at 1900 RPM was 33.4 mm/s². With the increase of engine speed, the displacement and velocity increased accordingly and reached the maximum of 0.044 mm and 5.2 mm/s at 1500 RPM, respectively. These findings prove a stepwise rise in vibration with increasing engine speed; the highest value being reached at 1500-1900 RPM. The results show the complicated dynamics of engine parts and give a clear meaning for the necessity of vibration analysis in order to reach better engine performance and to get rid of unstable oscillations. The drawl findings are selection of Chinese 150cc single-cylinder motorcycle engine I ne have the maximum vibration among those tested engines specifications as shown in the Table 4.

Lok	NA /	. engines	CHACITIC	otione

Vehicle	Engine Capacity (cc)	Cylinders	Bore (mm)	Stroke (mm)	Connecting Rod (mm)	Compression Ratio (CR)	Notes
Toyota	2500	6	75	75	140	10.5:1	Balanced for power & efficiency.
EXCELLE	1500	4	78	78	130	11.0:1	High CR for.
KIA	2700	6	77	86	145	10.0:1	Lower CR for higher torque.
ELANTRA	2000	4	80	80	135	10.8:1	Naturally aspirated, optimized CR.
JINYYEE	150	1	52	151	130	9.5:1	Low CR for air-cooled simplicity.

2.2.1. Kinematic Modeling of Piston Motion

The connecting rod feeds the piston, which transforms the power generated by the expanding gases inside the cylinder into linear motion, to the crankshaft. The instantaneous location of a piston is a crucial time-dependent performance parameter. The vector loop approach provides a mathematical explanation of the geometrical interactions between a crank, connecting rod, and piston. The crank radius, or the distance between the crank pin and the crankshaft center, and the connecting rod length, or the distance between the piston pin and the crank pin, are two of the variables that affect the piston's position. Additional variables include the connecting rod angle, which indicates the angle between the connecting rod and the vertical axis, and the crank angle, which is the crankshaft's rotation angle as shown in Fig. 8.

Using the crank mechanism shown in Fig. 9 the researchers developed the equation of crank mechanism. Additionally, the average piston Displacement velocity and acceleration.

$$x = l(\lambda^2 \sin^2 \theta/2) + r(1 - \cos \theta) \tag{1}$$

$$v_{\theta} = r\omega \left[\sin \theta + \frac{\lambda \sin 2\theta}{2} \right] \tag{2}$$

$$a_{\theta} = r\omega^2 [\cos \theta + \lambda \cos 2\theta] \tag{3}$$

3. Results and Discussion

Data was collected by numerical modelling and experimental procedures. Detailed physical data for fuel consumption, crankshaft speed and piston displacement in a wide range of operating conditions came from laboratory test on the single cylinder engine. To ensure reliability and consistency among data point we collected and analyzed data under the same conditions, more emphasis was given on speed and accuracy. During the entire experiment, data was recorded for 15 minutes as a minimum, to ensure that enough data points were collected to perform an analysis. To investigate thermal deflections and ensure the system has reached thermal equilibrium before data collection, the laboratory temperature was kept constant at 25 °C during the experiments. To consider variability, all measurements were performed at least three times. Each test, from setup, duration, atmospheric conditions and measurements, was performed in accordance with a uniform and replicable methodology. All apparatus were calibrated prior to each measurement to ensure accuracy. To exclude any possible influence of temperature and humidity, the experiments were conducted at a constant humidity of 40%. Throughout the experiment, temperature was continuously measured at 30-second or 1-minute intervals to track thermal fluctuations and make sure the entire system had reached thermal stabilization before the actual data collecting began. To model engine kinematics and forecast performance in various conditions, MATLAB simulations were run. The validity of the results was ensured by using experimental data to inform the simulation parameters as shown in Fig. 7. In agreement with earlier research (Zanganeh & Soleiman, 2021; Mnati et al., 2025; Niusha et al., 2021; Ranjbarkohan et al., 2010; Liss et al., 2024) [21, 5, 8, 22], connecting rod length, crankshaft radius, friction, lubrication, and cylinder number have a major impact on the vibration characteristics and overall performance of single-cylinder gasoline engines.

Engine performance and efficiency under various operating situations were examined using a dynamic model of engine kinematics created in MATLAB As shown in the Fig. 9. To obtain the kinematic equations, we first transformed the displacement, velocity, and acceleration equations into symbolic form. Next, we employed a numerical solver (Ode45 and Ode23) to solve the motion dynamics and modeled a dynamic system using the Simulink model. All these steps were carried out utilizing the sophisticated MATLAB approach, which analyzed and formulated their equations using the Symbolic Math Toolbox to make them simpler and more understandable before simulating numerical value. Both dataset's patterns, correlations, and uncertainties were thoroughly examined; these elements were crucial to the study's analytics and results. From the first parameter input to the calculations and output for every case, the MATLAB program's logic is demonstrated. Appropriate piston kinematics can be produced by calculating the crank and connecting rod lengths.

The process of evaluating the impact of increasing crank and connecting rod diameters on piston kinematics is outlined in the flowchart that follows. Crank radius, connecting rod length, crank angle range, and other important input parameters are specified at the start of the operation. Different engine configurations can be modeled thanks to this input phasing. The software iterates over each crank angle in the second stage

(computation), using the relevant kinematic equations to produce acceleration, velocity, and piston displacement. It is evident that Symbolic Math tools can be used to define these equations (very exactly). The data are looped through iteratively across all defined scenarios of crank and connecting rod dimensions. To sum up, data analysis is processed through many stages, where it is further clarified by the output visualization graphs and tables. In order to determine the ideal configuration, these outputs show how variations in dimensions affect the piston's motion. Graphs show patterns in how an engine's balance or efficiency changes with various factors during the course of the engine's operation, such as when comparing piston displacement.

It was able to guarantee a methodical approach by employing the MATLAB program's logic, which enabled a comprehensive examination of design trade-offs and gave engineers comprehensive information for decision-making. Although the numerical method offers a useful analytical framework, it may miss important details because it is based on the model's simplifications. These include simplifying engine shape, assuming stiff parts, neglecting friction and heat effects, and assuming unchanging attributes. Even though these presumptions are required for computational tractability, they may result in errors, especially under specific circumstances like high engine speeds or extremely high mechanical and thermal stresses. Nonetheless, the model provides a wealth of information for general analysis and engine performance and efficiency optimization within the bounds of typical operation.

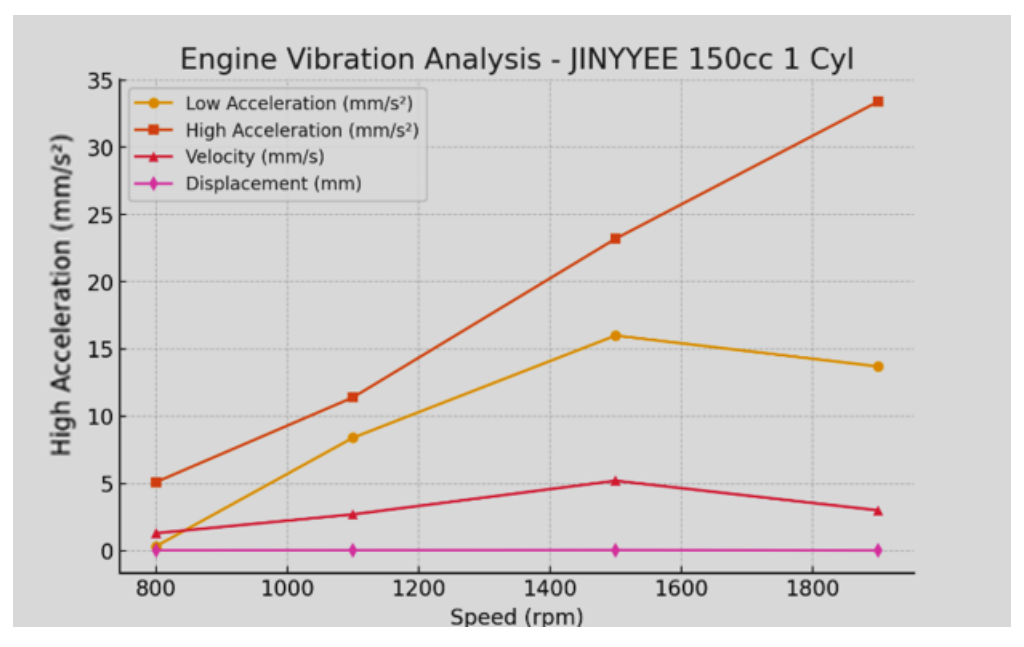


Fig. 2. Vibration analysis of single-cylinder engine

Fig. 2 illustrates key details regarding the dynamic behavior of the JINYYEE 150cc single-cylinder engine, commonly used in motorcycles. The vibration analysis graph highlights several measured parameters: low acceleration (orange), representing regular crankshaft rotation vibrations; high acceleration (yellow), indicating sudden combustion or impact-related vibrations; displacement (purple), measuring mechanical part movement in millimeters (mm); and velocity (red), indicating vibration intensity in mm/s. The engine was tested within the typical operating range for small engines, from 800 to 1800 RPM. Notably, at approximately 1400 RPM, a peak high acceleration of 30 mm/s² was observed, potentially indicating mechanical resonance or overload. Although displacement remained low, suggesting a solid mechanical structure, velocity increased linearly with RPM, confirming that vibration severity worsens at higher speeds.

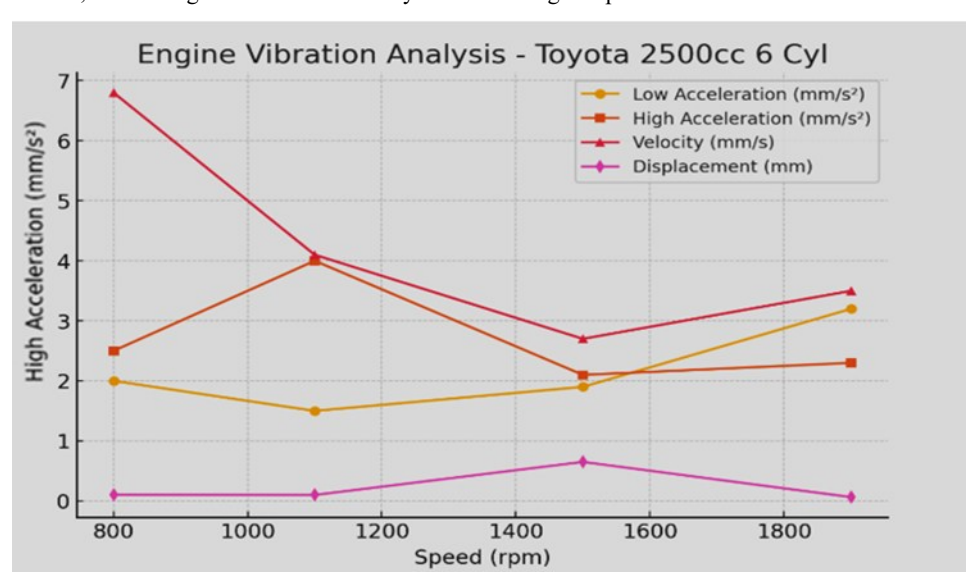


Fig. 3. Vibration analysis of six-cylinder engine

Fig. 3 compares vibration behaviors between engine types. The 6-cylinder engine exhibits lower vibration levels due to balanced forces across cylinders, whereas the single-cylinder engine shows significantly higher vibrations caused by the unbalanced force of a single power stroke. Regarding velocity and displacement, the 6-cylinder engine demonstrates smooth vibration distribution, minimizing overall oscillations. In contrast, the single-cylinder engine displays more pronounced vibration peaks due to its isolated combustion events. Across the RPM range, the 6-cylinder engine maintains smooth operation, while the single-cylinder variant vibrates more intensely, particularly at lower RPMs. This comparison highlights the natural balance advantage of multi-cylinder engines and the necessity of robust damping systems in single-cylinder designs.

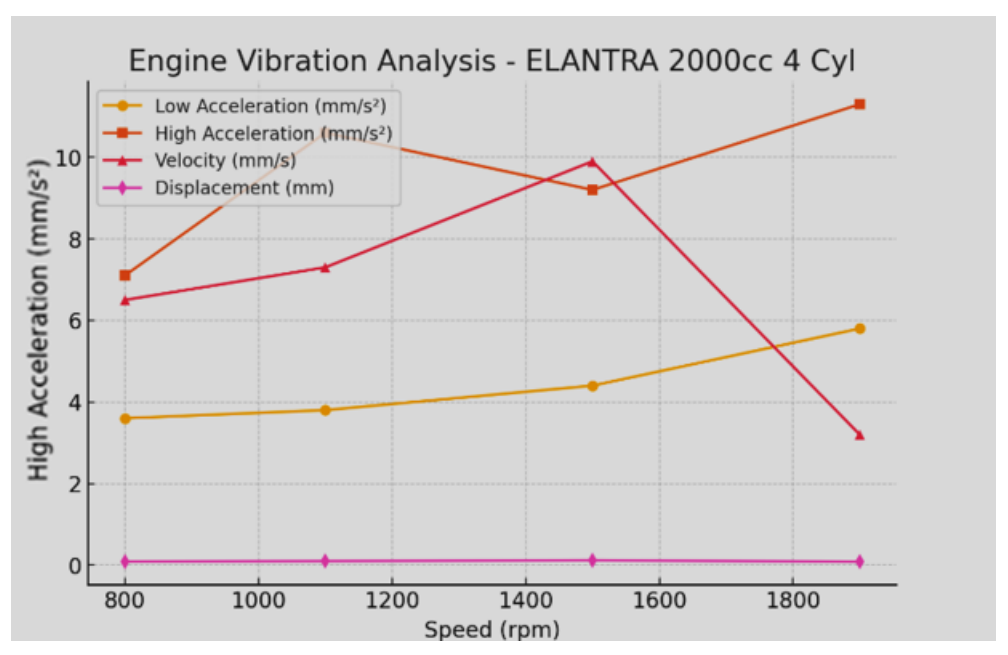


Fig. 4. Vibration analysis of four-cylinder engine

Fig. 4 presents the Hyundai Elantra's 2000cc 4-cylinder engine, which exhibits intermediate vibration characteristics relative to single- and six-cylinder configurations. Its acceleration values lie between those of smoother 6-cylinder engines and the more vibration-prone single-cylinder units, reflecting a balanced yet not perfectly uniform power delivery. In practice, the 4-cylinder engine demonstrates better vibration control than single-cylinder engines, especially around the critical mid-RPM range, approximately 1800 RPM. However, it does not match the superior smoothness of 6-cylinder engines, particularly under high acceleration or at elevated engine speeds. Displacement and velocity measurements further support this middle-ground behavior. Although the 4-cylinder configuration benefits from improved natural balance through its firing sequence, it lacks the overlapping power strokes characteristic of 6-cylinder engines. This makes the 4-cylinder a practical compromise, offering acceptable refinement while maintaining simpler mechanical design compared to larger multi-cylinder engines.

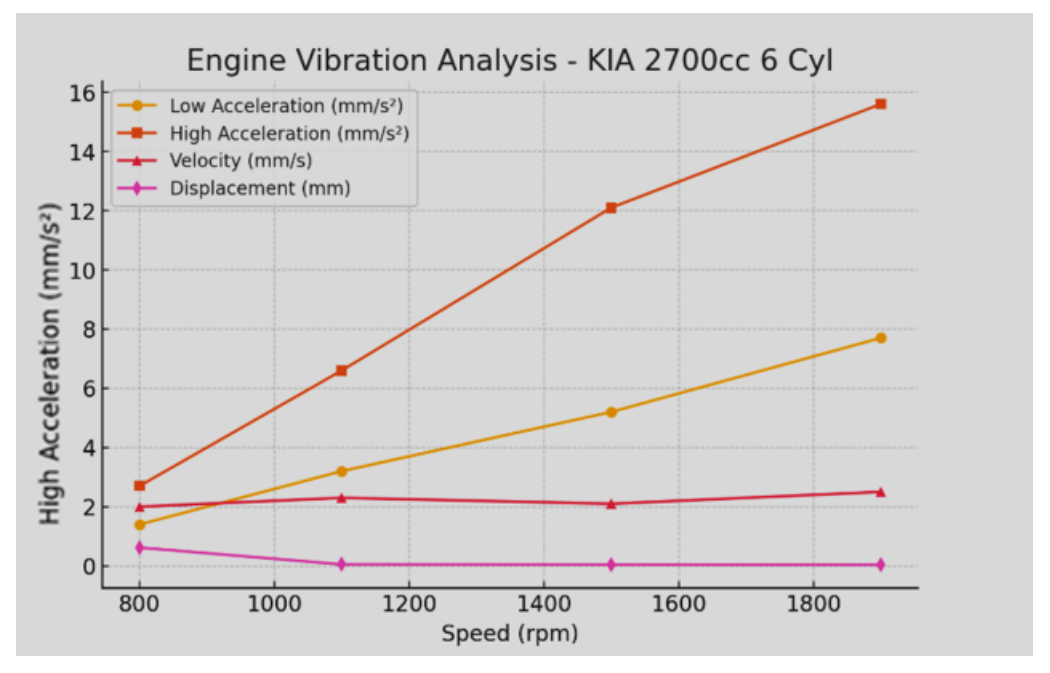


Fig. 5. Vibration analysis of six-cylinder engine

Fig. 5 depicts the vibration behavior of the KIA 2700cc 6-cylinder engine. This configuration demonstrates excellent vibration control, with acceleration values ranging between 2 and 8 mm/s² for both low and high acceleration. Velocity and displacement remain minimal, between 0 and 4 mm/s and mm respectively, indicating smooth operation across the entire tested RPM range from 800 to 1800 RPM. Compared to other engine types, this 6-cylinder unit shows superior vibration characteristics. Even at 1800 RPM, performance remains consistent without noticeable vibration. The smooth operation reflects the inherent balance advantages of 6-cylinder designs. In summary, while 4-cylinder engines offer a moderate compromise and single-cylinder engines show the highest vibration, the 6-cylinder engine achieves optimal refinement, explaining its preference for applications demanding smooth and quiet performance.

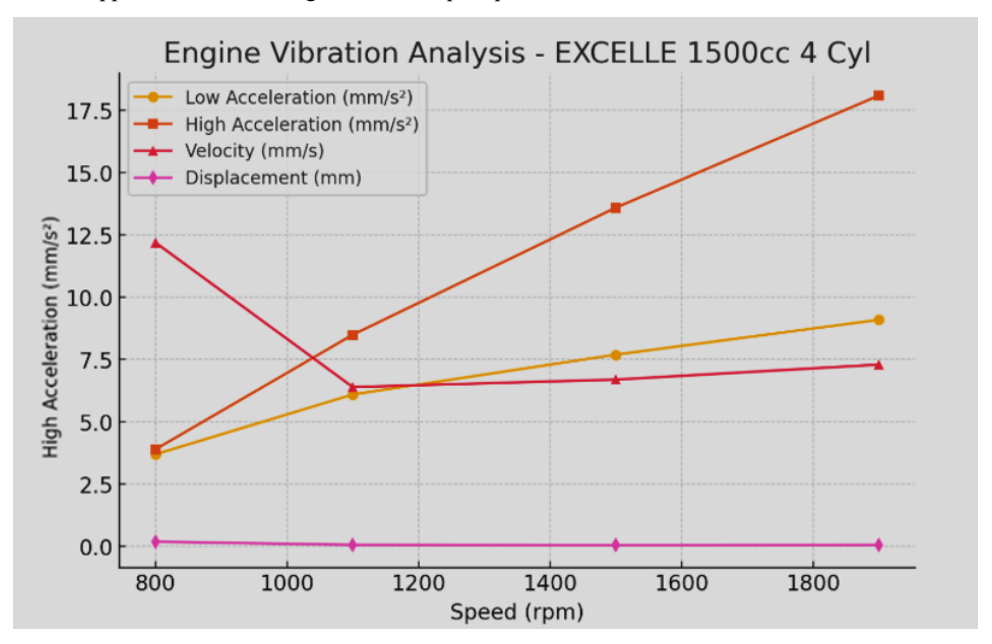


Fig. 6. Vibration analysis of four-cylinder engine

Fig. 6 analyzes a 1500cc 4-cylinder engine, which exhibits consistent behavior with moderate vibration levels between 7.5 and 17.5 mm/s² across the 1000 to 1800 RPM range. Although not as smooth as a 6-cylinder engine, this configuration offers significantly reduced vibration compared to single-cylinder designs. Engineering advances have enhanced the vibration control of these 4-cylinder units, making them compliant with modern vehicle standards. This balance of performance, cost-efficiency, and comfort explains the widespread adoption of 4-cylinder engines, particularly in vehicles prioritizing fuel economy and manufacturing efficiency without significantly compromising vibration control.

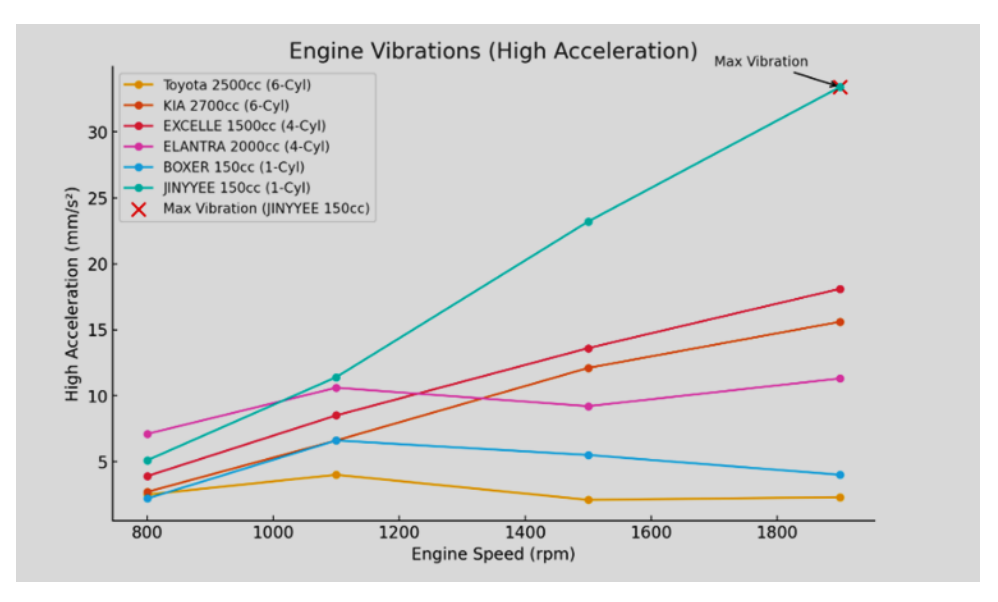


Fig. 7. Vibration analysis of all engine configurations

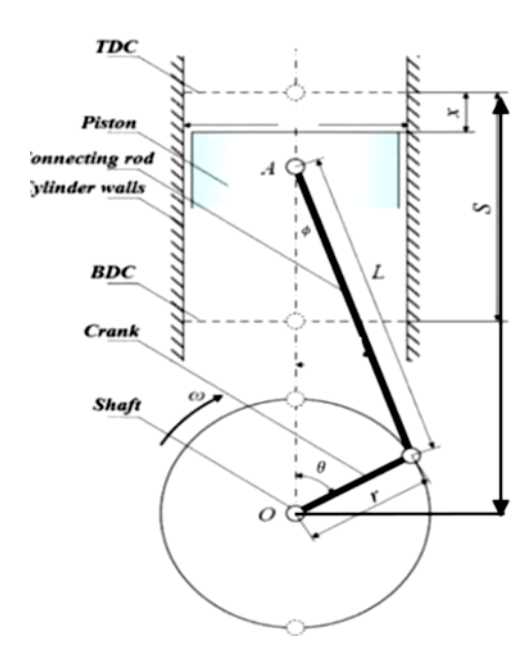


Fig. 8. Schematic of crank mechanism [31]

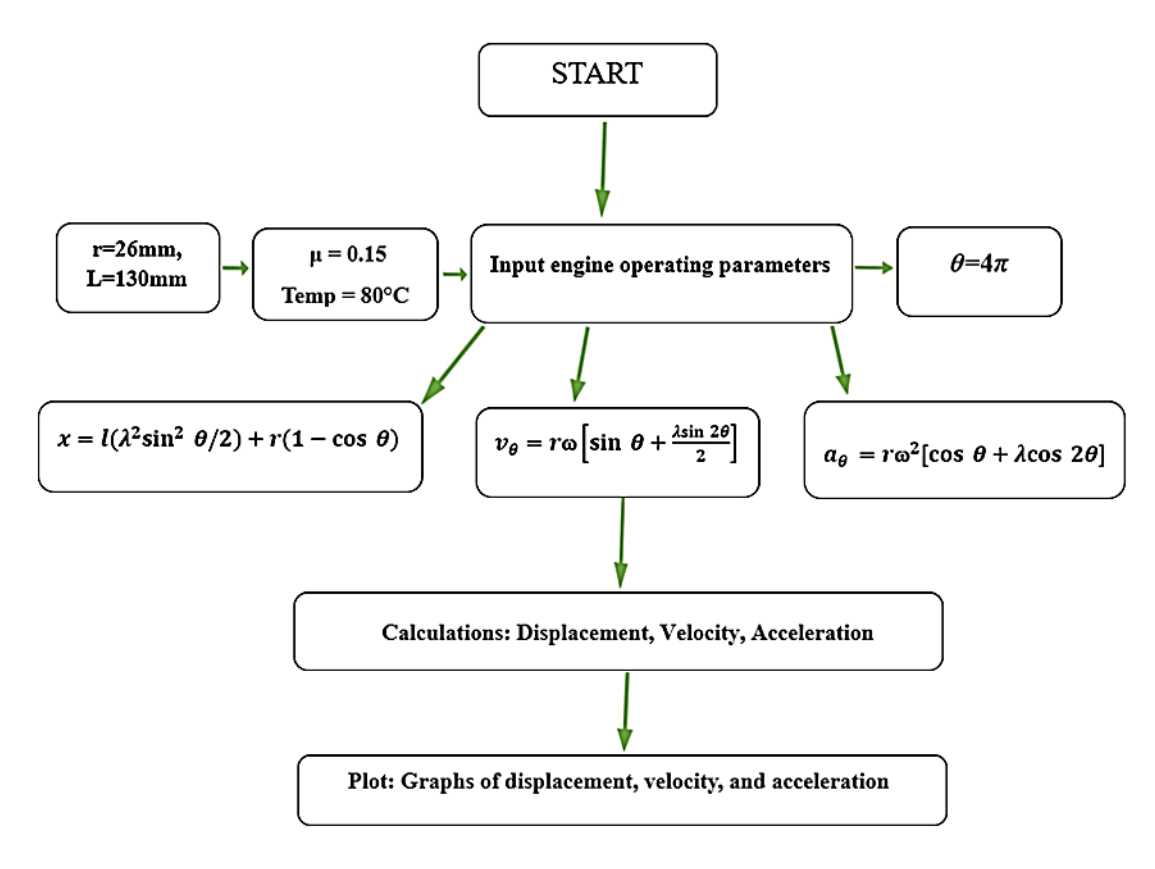


Fig. 9. Flowchart of the MATLAB program

Figure 7 further emphasizes the vibration control advantages of 6-cylinder engines. The Toyota 2500cc and KIA 2700cc units maintain high acceleration levels below 4 mm/s² across all RPM ranges, even at higher engine speeds. The KIA engine demonstrates exceptional damping consistency. In contrast, 4-cylinder engines represent a trade-off. Both the Elantra 2000cc and the Excelle 1500cc exhibit a gradual increase in vibration with RPM, typically between 4 and 8 mm/s², with the Elantra performing slightly better. The vibration profile of the JINYYEE 150cc single-cylinder engine stands out with the highest levels, peaking at 12 mm/s² at 1800 RPM. These pronounced fluctuations highlight the inherent imbalance in single-cylinder engines. Overall, the analysis reveals that vibration behavior is primarily influenced by the number of cylinders, with displacement size providing further stability benefits. Performance differences do become more obvious at high revolutions when you can get more readily available torque from 6-cylinder engines over a smaller configuration. These findings provide insights for the trade-off on engine design, which can contribute to the future powertrain balance, cost, and refinement optimization.

This relation between crankshaft angle (x-axis) and piston displacement (y-axis) is shown in Fig. 10 for a crank radius of 130 mm. At 180° of crankshafts angle, the displacement curve follows a modified sinusoidal trend, and it can ideally achieve a maximum of 260 mm (twice the crank radius). This is the relationship upon which engine kinematics is based and is essential for the accurate measurement of stroke and computing compression ratio. What is more, important signaling is created for monitoring the mechanical soundness and working state of the connecting rod assembly.

These findings are useful for improving the engine performance, specifically when it comes to the redesign of combustion chambers and the analysis of the dynamic balance of the reciprocating masses. It should be mentioned that actual displacement curves are frequently affected by small deviations from this ideal curve due to a variety of influences, such as con-rod length, non-linear acceleration profiles, and the elastic behavior of engine structures when loaded.

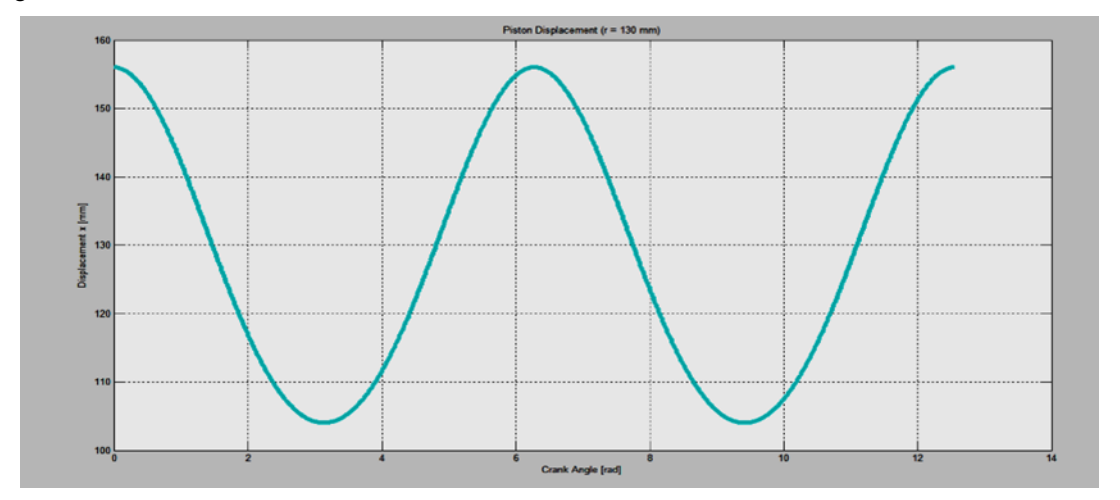


Fig. 10. A representation of piston displacement

The behavior of the piston with respect to the velocities is shown on Fig. 11. The black curve is the curve for ideal case, whose maximum is 30 mm/rad and represents the theoretical limitation. The red line includes the friction effects and has compared with the black line a slower speed (15–20%) that stands out specifically between 10 and 12 radians. Thermal effects denoted by the green curve slows the nozzle velocity 10–15\% and generates an asymmetric macropulse with the leading and trailing edges of the package softened for the accelerating phases. The blue curve, which represents combined influences of friction and thermal influences, shows the largest effect, with complete velocity reduction of 25–30%, and maximum value restricted to 21 mm/rad.

The results indicate that friction plays a dominant role in the initial stages of crank rotation (3–11 radian) and thermal distortions dominate in the power stroke (11–15 radian). The interactive friction and heat phenomena generate non-linear and non-additive performance deterioration, which is higher than that of individual components. These results are valuable as part of the optimisation of piston ring design and the development of thermal management strategies, as well as for condition monitoring, predictive maintenance and to overall further improvement of engine performance.

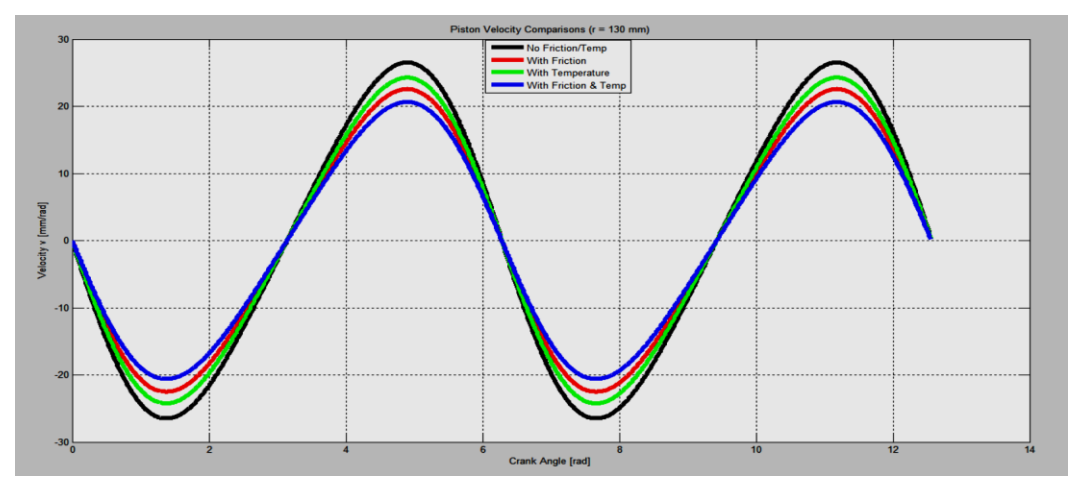


Fig. 11. A representation of piston velocity

The experimental acceleration profiles, presented in Fig. 12, provide valuable information about the behavior of the piston over different operating conditions. The black curve, which presents the ideal case, is a sinusoidal curve with ideal peak acceleration of -40 and +30 mm/µs² during the exhaust and compression strokes, respectively. The red curve, representing the effect of friction, illustrates a 15–20% energy dissipation at around the mid-stroke area. Thermal distortions are visible in the green curve, particularly during the power stroke between 10 and 14 radians, reflecting that differences exist because of non-uniform temperature and thermal expansion.

For the blue curve considering the simultaneous influence of friction and thermal effects, the largest deviation is observed. The curve exhibits waiting-time-dependent non-linearity, including phase lag, as well as strong suppression of the peak acceleration to $\approx 25 \text{ mm/}\mu\text{s}^2$ in the critical

10-12 radians range where the peak stress, thermal gradients, and frictional forces come together. These findings also clearly demonstrate the necessity to improve cooling systems and piston ring layouts, especially in areas with higher temperature and mechanical loads. They also emphasize the necessity of reorganization of engine control strategies in the presence of non-linear phase transitions under dynamic conditions.

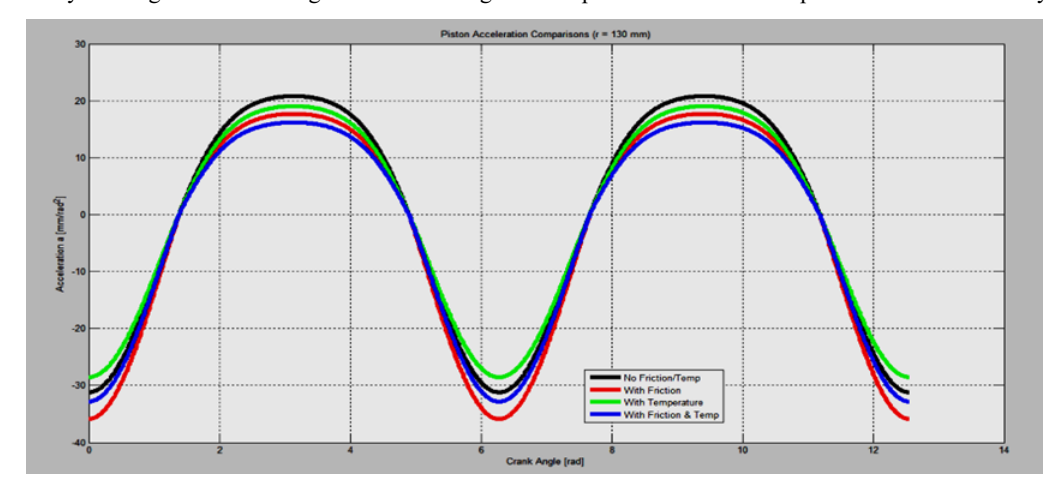


Fig. 12. A representation of piston acceleration

4. Conclusion

In this study, a MATLAB based model that governed the kinematic behavior of an internal combustion engine was proposed. Vibration features were investigated experimentally of four-stroke engines at different engine speeds. Based on the analysis of the results, the following conclusions are possible:

- Increasing the connecting rod length of l results in improved piston displacement, velocity, and acceleration.
- Displacement increases linearly with rod length, enhancing the overall piston stroke efficiency.
- Longer rods provide higher maximum velocities and accelerations, improving engine performance, especially in high-speed conditions.

Impact of Environmental Effects (Friction and Temperature):

- Friction reduces both velocity and acceleration by approximately 15% for all rod lengths
- Temperature reduces velocity and acceleration by 8.5%, affecting engine efficiency across all rod lengths.
- The combined effect of friction and temperature results in the most significant performance degradation, reducing velocity and acceleration by about 22%.

The Toyota 6-cylinder engine is among the most dependable, low-vibration, and long-lasting. The Toyota 2500 and BOXER 150CC engines displayed the lowest vibrations (1.4 mm/s² at 800 rpm), suggesting exceptional stability.

Increasing the length of the connecting rod significantly improves piston performance by increasing displacement, velocity, and acceleration. Environmental effects, such as friction and temperature, have a notable impact on performance, with the combined effect causing the most degradation.

Future work should look at the effects of optimal engine performance, a balance between rod length, friction, and temperature effects. Dynamic Balance Optimization: A thorough examination of how connecting rod length affects combustion efficiency while taking into account the intricate connection between mechanical friction and inertia. Development of nano-lubricants that can tolerate high temperatures and lower friction coefficients by up to 40% in comparison to traditional oils is known as advanced lubrication systems. Smart Thermal Management: Using Phase Change Materials to absorb excess heat during peak load operation, hybrid cooling systems are designed. Vibration analysis involves the use of composite materials with better vibration-damping capabilities, including synthetic rubber bonded with carbon fiber, in conjunction with ongoing crankshaft balance monitoring. In-depth Wear Studies: Scanning Electron Microscopy is used for microscopic surface examination and accelerated testing to replicate harsh operating conditions. Advanced Modeling: Creating 3D computer simulation models that take into consideration the interactions of mechanical, thermal, and dynamic factors.

Acknowledgment

We express our gratitude to the Technical Institute / Baquba, Middle Technical University, Baghdad, Iraq for the support that were useful in this study.

References

- [1] Y. Xiang, J. Yao, Q. Zhou, S. Qian, and S. Wang, "Research on Experimental Method for Obtaining Independent Combustion Noise of Internal Combustion Engine," Shock Vib., vol. 2018, Article ID 2413831, 14 pages, 2018, https://doi.org/10.1155/2018/2413831.
- [2] C. H. Cheng, Y. H. Tan, and T. S. Liu, "Experimental and Dynamic Analysis of a Small-Scale Double-Acting Four-Cylinder-Type Stirling Engine," Sustainability, vol. 13, p. 8442, 2021, https://doi.org/10.3390/su13158442.
- [3] F. Consuegra, A. Bula, W. Guillín, J. Sánchez, and J. Duarte Fore, "Instantaneous in-Cylinder Volume Considering Deformation and

- Clearance due to Lubricating Film in Reciprocating Internal Combustion Engines," Energies, vol. 12, p. 1437, 2019, https://doi.org/10.3390/en12081437.
- [4] F. Yu, J. Xie, and Z. M. Xu, "The vibration reduction design of single-cylinder engine based on the balance shaft," Vibroeng. Procedia, 2019, https://doi.org/10.21595/vp.2019.20651.
- [5] H. M. Mnati, M. Hammami, O. Ksentini, M. S. Abbes, M. Haddar, and M. M. Hanon, "Kinematic and vibration analysis of a single-cylinder engine: Effects of connecting rod length, fuel type, and engine speed," Int. Rev. Appl. Sci. Eng., 2025, https://doi.org/10.1556/1848.2025.00944.
- [6] H. Nigus, "Kinematics and Load Formulation of Engine Crank Mechanism," Mech. Mater. Sci. Eng. J., Magnolithe, 2015, https://doi.org/10.13140/RG.2.1.3257.1928.
- [7] M. Lučić, "Kinematic analysis of the slider-crank mechanism of an internal combustion (IC) engine using modern software," Mech. Agric. Conserv. Resour., vol. 68, no. 1, pp. 11–17, 2025.
- [8] N. F. Zanganeh, G. Shahgholi, and S. Agh, "Studying the effect of balancer on engine vibration of Massey Ferguson 285 tractor," Acta Technologica Agriculturae, vol. 24, no. 1, pp. 14–19, 2021, https://doi.org/10.2478/ata-2021-0003.
- [9] M. Viswanath, S. Ajay, S. Bharathraja, R. Deepika, and J. J. Ramnath, "Design and analysis of piston on different materials using CAE tools," Int. J. Eng. Res. Technol. (IJERT), vol. 9, no. 10, ETEDM-2021.
- [10] H. Zhang and J. Wu, "Thermal strength and transient dynamics analysis of a diesel engine piston," J. Vibroeng., vol. 16, no. 5, Aug. 2014.
- [11] M.-N. Pham, C.-J. Yang, J.-H. Kim, and B.-G. Kim, "Transient Structural Analysis of Piston and Connecting Rods of Reciprocating Air Compressor Using FEM," J. Korean Soc. Mar. Environ. Saf., vol. 23, no. 4, pp. 393–399, Jun. 2017, https://doi.org/10.7837/kosomes.2017.23.4.393.
- [12] M. Ranjbarkohan, M. Rasekh, A. H. Hoseini, K. Kheiralipour, and M. R. Asadi, "Kinematics and kinetic analysis of the slider-crank mechanism in Otto linear four-cylinder Z24 engine," J. Mech. Eng. Res., vol. 3, no. 3, pp. 85–95, Mar. 2011.
- [13] P. Horváth and J. Égert, "Dynamic analysis of a one-cylinder engine crankshaft," Acta Technica Jaurinensis, vol. 8, no. 4, pp. 280–295, 2015, https://doi.org/10.14513/actatechjaur.v8.n4.379.
- [14] F. Alkhatib and A. K. Dhingra, "Shape Optimization of Engine Mounts for Enhanced Vibration Isolation," Proc. ASME Int. Mech. Eng. Congr. Expo., IMECE2013-64476, 2013, https://doi.org/10.1115/IMECE2013-64476.
- [15] J. Beckers, T. Verstraten, B. Verrelst, F. Contino, and J. Van Mierlo, "Analysis of the Dynamics of a Slider-Crank Mechanism Locally Actuated with an Act-And-Wait Controller," Mech. Mach. Theory, 2020, https://doi.org/10.1016/j.mechmachtheory.2021.104253.
- [16] J. Chen, R. B. Randall, N. Feng, B. Peeters, and H. Van der Auweraer, "Simulating bearing knock in an IC engine," Proc. 20th Int. Congr. Sound Vib. (ICSV), vol. 4, pp. 3321–3328, 2013.
- [17] H. Zheng, H. Zhou, C. Kang, Z. Liu, Z. Dou, J. Liu, B. Li, and Y. Chen, "Modeling and prediction for diesel performance based on deep neural network combined with virtual sample," Sci. Rep., 2021, https://doi.org/10.1038/s41598-021-96259-x.
- [18] E. Armentani, F. Caputo, L. Esposito, and R. Citarella, "Multibody Simulation for the Vibration Analysis of a Turbocharged Diesel Engine," Appl. Sci., vol. 8, p. 1192, 2018, https://doi.org/10.3390/app8071192.
- [19] M. Madamedon, "The Characteristics of Instantaneous Angular Speed of Diesel Engines for Fault Diagnosis," Ph.D. thesis, Univ. Huddersfield, 2018. http://eprints.hud.ac.uk/id/eprint/34553.
- [20] R. Tailony, "New Modeling Approach for Engine Cold Testing Driveline Torsional Vibration Analysis with Increased Accuracy," Am. J. Mech. Eng., vol. 5, no. 4, pp. 156–160, 2017.
- [21] Farrokhi Zanganeh N, Shahgholi G, Agh S. Studying the effect of balancer on engine vibration of Massey Ferguson 285 tractor. Acta Technol Agric. 2021; 24:14–9.
- [22] Liss, M., Martynyuk, V., & Martinod, R. (2024). Dynamic analysis of an internal combustion engine made in downsizing technology. MATEC Web of Conferences, 391, 01009. https://doi.org/10.1051/matecconf/202439101009.
- [23] Marwa N. Kareema, Adel M. Salih, (2020). Engine performance with diesel-biodiesel blends fuel and emission characteristics. Engineering and Technology Journal, 38(A05), 779-788. https://doi.org/10.30684/etj.v38iA.1420.
- [24] Marzec, P., & Kubica, G. (2024). Dynamic parameters of a car with a SI engine fueled with LPG/DME blends. Combustion Engines, 198(3). https://doi.org/10.19206/CE-2024-03.
- [25] Uski, O. J., Rankin, G., Wingfors, H., Magnusson, R., Boman, C., Lindgren, R., Muala, A., Blomberg, A., Bosson, J. A., & Sandström, T. (2024). The toxic effects of petroleum diesel, biodiesel, and renewable diesel exhaust particles on human alveolar epithelial cells. J. Xenobiot., 14(4), 1432-1449. https://doi.org/10.3390/jox14040080.
- [26] Noga, M., & Mareczek, M. (2020). Vibrations problems in the range extender developed for an electric light commercial vehicle. MATEC Web of Conferences, 020034.
- [27] Daud, S., Hamidi, M. A., Mamat, R., & Nafiz, D. M. (2023). A prediction of graphene nanoplatelets addition effects on diesel engine emissions. International Journal of Automotive and Mechanical Engineering, 20(3), 10758-10766. https://doi.org/10.15282/ijame.20.3.2023.17.0831.
- [28] Zuxin Chen, Fei Wang*, Shan Zeng, Yancong Lin (2025). Dynamic Similarity Optimization Design of an Aero-Engine Open Journal of Applied Sciences, 2025, 15(4), 773-783 https://www.scirp.org/journal/ojapps.
- [29] Nkrumah Jacob Kwaku, Baba Ziblim, Sulemana Yahaya, Sherry Kwabla Amedorme (2023) Modal and Thermal Analysis of a Modified Connecting Rod of an Internal Combustion Engine Using Finite Element Method Modeling and Numerical Simulation of Material Science, 2023, 13, 29-49 https://www.scirp.org/journal/mnsms.
- [30] Suzara Rayanne de Castro Sena, André Luis Oliveira de Almeida, Leonara Luizza da Costa Leite, Jean Gustavo de Melo Araujo, Eduardo Lins de Barros Neto, Camila Gambini Pereira (2021). Effect of Blends Gasoline with Oxygenated Additives in the Performance of Internal Combustion Engine Journal of Power and Energy Engineering, 2021, 9, 1-9 https://www.scirp.org/journal/jpee.
- [31] S. G. Chernyi, P. Erofeev, B. Novak, and V. Emelianov, "Investigation of the mechanical and electromechanical starting characteristics of an asynchronous electric drive of a two-piston marine compressor", J. Mar. Sci. Eng., vol. 9, p. 207, 2021, https://doi.org/ 10.3390/jmse9020207.